Interfacial Mass Transport Effects in Composite Materials[1]

Jan W. Nowok[2]

---

[1] Paper presented at the Thirteenth Symposium on Thermophysical Properties , June 22–27, 1997, Boulder, Colorado, USA.

[2] Materials Technologies, University of North Dakota, Energy & Environmental Research Center, PO Box 9018, Grand Forks, ND 58202, USA.

ABSTRACT

It has been suggested that induced atomic layering transitions at the liquid metal–substrate interface may contribute to the mass transport process in dissimilar materials, along with the energetics of wetting associated with $\gamma_{SV} - \gamma_{SL}$, where, γ_{SV} and γ_{SL} represent solid surface and solid–liquid interfacial energies, respectively. A quasi-solidlike skin is thought to form during presolidification of the liquid on the substrate. The formation of this quasi-solidlike skin is activated by electrons transferred from the solid to the liquid or vice versa, depending on a work function difference. The electric double layer and the effective pairwise interactions in the presolidified liquid are strongly dependent upon the nonstoichiometry of solid materials. TiN_x and $Ti(N,O)_x$ ceramics and liquid Ti were selected to examine surface layering and the apparent surface diffusion of the liquid.

KEY WORDS: diffusion coefficient; interfacial tension; wettability.

1. INTRODUCTION

The main factors that affect material processing and, further, the nature of a metal–ceramic interface, its structure, and morphological stability are liquid surface mass transport related to adhesional wetting (physical effect) and reactive wetting (chemical effect) [1].

The energetics of wetting driven by capillary imbalance forces are generally believed to control interfacial mass transport rather than the strong layering forces generated by the electrostatic contribution of adsorbed multilayers of a liquid phase on a substrate [2] and/or viscoelastic dissipation in the wetting ridge of the substrate near the triple point [3]. In practice, an increase in mass transport behavior in dissimilar materials is seen as the effect of liquid–solid reactions and/or alloying either the substrate or adsorbate with other materials [4]. However, attractive pairwise interactions between atoms in a liquid and solid via the well-known Lennard–Jones wall potential may be also involved in wetting of the solid [5]. The objective of this work is twofold: 1) to extend the prior energetic analysis of mass transport phenomena to wetting behavior between liquid metal and the quasi-solidlike skin resulting from the presolidification of liquid on nonstoichiometric solids on a scale of interatomic distance and 2) to provide experimental verification of our concept. The formation and stability of quasi-solidlike skins seem to depend on changes in the electronic states of the contacting surface layers of both the substrate and the liquid, which can be represented by a work function difference, $\Delta\phi$, between liquid and solid (or more rigorously, in the Fermi energy difference), and a

difference in the electronic densities of states, Δn. These parameters are very sensitive to the stoichiometry and composition of the crystalline phase.

The concept of a stratified interface structure is derived from studies on density changes in liquids at free surfaces, premelting of certain crystalline facets, the double layer structure formed in metal–solvent systems, and the physics of wetting in three-dimensional systems with planar symmetry [6–9]. Our concept of the role of nonstochiometry and composition on surface mass transport was verified by performing wettability tests of liquid titanium on nonstoichiometric TiN_x and $Ti(N,O)_x$ ceramics and correlating those results with the electronic state of the ceramics.

2. LIQUID–SOLID INTERFACES AND APPARENT SURFACE DIFFUSION

At present, no model is able to describe satisfactorily the processing of metal–matrix composites (MMCs). It is our thesis that MMC processing is crucially dependent on surface diffusion in the wetting ring near the triple point, solid–liquid–vapor, and driven by 1) the energetics of wetting: $\gamma_{SV} - \gamma_{SL}$ introduced by the liquid metal–substrate interaction (where γ_{SV} and γ_{SL} represent the solid surface and solid–liquid interfacial energies, respectively); 2) the energetics of wetting arising at the liquid metal–quasi-solidlike skin interface (Fig. 1; see details below); and 3) the intrinsic stresses at the interface resulted from the formation of quasi-solidlike skin, which may change the interfacial surface energy of the substrate.

In previous work, we attempted to understand the physical and chemical origins of surface mass transport in metal–metal and metal–carbide systems [1]. We introduced the apparent surface diffusion parameter given by

$$D_S + D_r = (\gamma_{LV}/\eta)\ L\ \lambda\ \cos\theta_e\ [m^2/s] \text{ at } T = \text{constant}$$

where D_S and D_r represent diffusion driven by adhesional forces and reaction-enhanced diffusion of atoms from a liquid, respectively; γ_{LV}/η is the surface tension-to-viscosity ratio for liquid metal; λ is the geometrical factor when anisotropic properties of a substrate result mostly from the roughness of the solid surface; L represents the average atomic/ionic distances in a solid; and θ_e corresponds to a wettability angle at thermodynamic equilibrium in a liquid–solid system. The equation provides a good estimation of surface diffusion for liquid metal–solid metal systems; however, some large $D_S + D_r$ values for liquid metals on carbides seem to be suspect and are likely caused by a the large difference in L between a solid and liquid (Table I). The L in carbides corresponds to the distance between either carbon or metal atoms in the B1 structure calculated in two crystallographic directions, [110] and [100] (Fig. 2), and in liquid metals related to the nearest-neighbor distance [1]. A straightforward strategy to correct the $D_S + D_r$ property is to assume that the layering transition in liquid metal on a substrate occurs with the formation of the quasi-solidlike metal interface. It is expected that the new L for the quasi-solidlike interface will be between that of a liquid metal and a solid substrate and will not depend on crystallographic directions. In liquid metal–solid metal systems, the misfit in L from metal to metal is low [1]; however, it is high between metal and

oxide/carbide/nitride. Thus, the layering transition at the interface will reduce the misfit between the substrate and liquid phase.

3. LAYERING TRANSITIONS AT THE LIQUID–SOLID INTERFACE

To understand the wetting phenomena at the liquid metal–solid interface, one must consider metal liquid structure at melting temperature. Liquid metals are considered a two-component fluid in structure, one composed of ion cores and another composed of nearly free conduction electrons. The ion-electron forces constructed from pseudopotentials depend strongly on changing electron density at the Fermi energy level [18]. The partial delocalization of electrons near an interface caused by electron transfer either from solid to liquid or liquid to solid leads to a change in effective pairwise interaction between ions. The energy of this process is not conserved. In transition metals, electrons from the d-bands seem to play a crucial role [19].

As a consequence of the partial delocalization of conduction electrons, a close-packed liquid layer with higher packing density forms on a substrate, exhibiting a layering transition, which will extend into the bulk liquid with an exponential decay. This process leads to the ordering of atoms near the interface and a sudden change in melt structure such as observed in a quasi-solidlike skin in a solid metal near its premelting temperature. The structure of a thin, coherent phase can be either amorphous or similar to that of a superlattice in alloys [20]. In this process, a fraction of the full entropy is liberated. It is likely that the ordering mechanism of atoms in a liquid phase at the interface is opposite to the disordering or deconstruction transition in metal crystals below their melting

temperature [21]. The existence of layering transitions for metals with low-index faces has already been predicted with density functional calculations. For these systems, the interface states have identical structure parameters. However, at a liquid–solid interface in dissimilar materials, electrons behave as if they belong to two different phases composed of two different structure parameters with some lattice misfit.

The transition from a disordered liquid to an ordered one in quasi-solidlike skins should be initiated by the electronic states of the contacting phases of both the substrate and liquid, described by a work function difference, $\Delta\phi$, and the difference in the electronic densities of states, Δn. The difference between work functions, $\Delta\phi = W_m - W_s$ (where W_m and W_s represent work functions of the liquid metal and substrate, respectively), gives rise to an electric dipole layer. The quasi-solid-like skin can support a potential difference, but will be transparent to the flow of electrons between liquid metal and substrate such as it is in a metal-semiconductor junction with an interfacial layer and interface states. However, the quasi-solidlike skin may reduce the $\Delta\phi$ of a substrate. It has already been demonstrated that the work function of α-SiC can be reduced from 4.5 to 2.9 eV when the thickness of deposited europium increases from 0 to 20 Å [22]. Electron work functions usually decrease as temperature rises, mainly as a result of lowering the material's density. Unfortunately, no measured values for work functions in liquid metals, except for alkalies, are available in the literature. Therefore, in this discussion, we use values of ϕ determined for solid phases.

Generally, work function is highly sensitive to perturbation at a material's surface resulting from crystallographic orientation, nonstoichiometry, and adsorption of gases. Transition metal carbides and nitrides typically exist as nonstoichiometric, with either ordered or disordered vacancies in the nonmetallic sublattice. The presence of nonmetal vacancies results in an increase in the density of states at the Fermi energy level. When carbon vacancies are formed, some charge is transferred to the vacancy sphere from the C2p bands, lowering the Fermi energy. Therefore, the vacancies cannot be considered electron traps [23]. However, they can control the interface potential and donate electrons to other materials. The decreasing copper contact angle θ_e on nonstoichiometric TiC_x ceramics with increasing apparent surface diffusion parameters is good evidence of the role of electron transfer in the wettability process (Table I).

The increase in work function in carbides with oxygen content (Table I) creates new energies in the surface state, which in particular cases may reduce the probability of layering transitions and, simultaneously, of the wetting ability of oxidized carbides. Usually, oxygen atoms occupy carbon vacancies and are involved in the increase in the ionic character of bonds [24]. Also, it has been suggested that thin oxide films formed on liquid metals inhibit the wettability of ceramic surfaces by these metals [25].

4. EXPERIMENTAL

A series of TiN_x and $Ti(N,O)_x$ films formed from a $TiCl_4$, N_2, H_2, and (N_2 + O_2) gas mixture was deposited on alumina ceramics at 1073 K for 5 hr at atmospheric pressure, according to the procedure described in Dekker et al. [26]. These conditions

were selected because they offer a reasonable deposition rate and low chlorine content in films. The TiN_x films with two different nonstoichiometries controlled by the ratio of N_2 to H_2 and two $Ti(N,O)_x$ films with different nitrogen and oxygen content were prepared. The N_2 and H_2 gases were first purified in alkaline pyrogallol and dried over silica gel and further over a copper and palladium catalyst. $TiCl_4$ concentration in flowing N_2 and H_2 (70/30) corresponded to its vapor pressure over liquid at 300 K. The film thickness were determined using a multiple interfometer. All of the films obtained were thicker than 1000 nm. Phase analysis and interatomic distances were determined by x-ray diffraction (XRD) analysis at room temperature.

The films were characterized by electron spectroscopy for chemical analysis (ESCA) using a PHI 595 multiprobe depth profiling. A Mg Kα x-ray source and a double-pass cylinder mirror electron analyzer were used for excitation. Peak positions were corrected by assuming that the very weak C 1s photoelectron line present for each sample was at 284.6 eV. All measurements were taken at room temperature. Scanning electron microscopy was applied for morphology tests.

Wettability tests of liquid titanium on TiN_x and $Ti(N,O)_x$ films were done using the sessile drop technique in high-purity Ar at 1973 K [1].

5. RESULTS AND DISCUSSION

Table II lists the results of both stoichiometry and x-ray structural analysis for TiN_x and $Ti(N,O)_x$ samples. There is a characteristic trend in changes of the lattice parameter

for TiN_x, which decrease from 0.4240 ± 0.0003 nm to 0.4225 ± 0.0002 nm with a nitrogen content deficit.

The decrease in lattice parameter in TiN_x films results from the formation of nitrogen vacancies. The $Ti(N,O)_x$ samples contain two phases based on η-Ti_3N_{2-x} and ζ-Ti_4N_{3-x} . These phases are stable only above 1373 K and are formed by a martensitic diffusionless transformation of TiN_x during heat treatment above that temperature for a long period of time, up to 330 hr [28,29]. Their formation at temperatures as low as 1173 K are likely caused by a changes in TiN_x crystal symmetry as a result of nitrogen vacancies substitution by oxygen.

Figure 3 illustrates XRD patterns, in the range of 36–44 two-theta angles for three films: two belong to the TiN_x phase, and one is composed of TiN_x, and η-Ti_3N_{2-x} plus ζ-Ti_4N_{3-x} phases. In the two $Ti(N,O)_x$ films, we did not detect any peaks belonging to titanium oxide(s). The size of the titanium nitride grains was between 1 and 3 mμ.

Table III lists the measured contact angles of liquid titanium on TiN_x and $Ti(N,O)_x$ films, as well as on Al_2O_3 ceramic at 1973 K taken from the literature [30]. The value of the contact angles depends significantly on the stoichiometry and composition of the titanium nitride. The nitrogen vacancies reduce contact angles, and oxygen impurities increase the θ_e. These results are consistent with our theoretical model of mass transport through the liquid phase, which suggests that nitrogen vacancies lower the electron work function in TiN_x ceramics, which may activate the formation of the quasi-solidlike interface which, in turn, should promote the mass transport of liquid metal. On the other

hand, contaminants such as oxygen increase the work function of TiN_x ceramics to a value close to the work function of titanium metal, and this simultaneously causes a decrease in the mass transport process. This conclusion is reflected in the $D_S + D_r$ values (Table III).

The above results suggest that in investigating the wetting phenomenon of liquid metals, the electronic component generated at the metal–substrate interface must not be neglected. Its physical origins result from differences in both the electron work function and the electronic densities of states. Surface mass transport at the triple point (solid–liquid–vapor) may proceed by lateral diffusion of adatoms on the quasi-solidlike skin driven by the energetics of wetting, a process that can be assigned to physical effect. The chemical effect that causes the formation of new phases, which may reduce interface energy, is not discussed in this manuscript.

6. ACKNOWLEDGMENTS

The author would like to thank the U.S. Department of Energy for its partial support of this work through funding of contract No. DE-FC21-93MC30097. Thanks are also expressed to Dr. Catherine A. O'Keefe for XRD tests.

7. REFERENCES

1. J.W. Nowok, *Mater. Sci. Eng. A*, accepted for publication.
2. A.A. Cernov and L.V. Mikheev, *Phys. Rev. Lett*. **60**: 2488 (1988); *Physica* **A157**: 1042 (1989).
3. A. Carre, J-C. Gastel and M.E.R. Shanahan, *Nature* **379**: 432 (1996).
4. R.M. Cannon, E. Saiz, A.P. Tomsia and W.C. Carter, *Met. Res. Soc. Symp. Proc.* **357**: 279 (1995).
5. F.F. Abraham, in *CRC Critical Reviews in Solid State and Materials Sciences*, May 1981, p. 169.
6. M. Hasegawa and T. Ichikawa, *J. Phys. (Condensed Matter)* **3**: 2769 (1991).
7. M.J. Regan, E.H. Kawamoto, S. Lee, P.S. Pershan, N. Maskil, M. Deutsch, O.M. Magnussen and B.M. Ocko, *Phys. Rev. Letters* **75**: 2498 (1995).
8. L. Bosio, R. Cortes, G. Folcher and M. Froment, *J. Electrochem. Soc.* **139**: 2110 (1992).
9. J.R. Henderson, *Phys. Rev.* **E50**: 4836 (1994).
10. R. Warren, *J. Mater. Sci.* **15**: 2489 (1980).
11. R. Standing and M. Nicholas, *J. Mater. Sci.* **13**: 1509 (1978).
12. J.W. Nowok, *Acta Metall. Mater*. **42**: 4025 (1994).
13. V. Moisy-Maurice, N. Lorenzelli, C.H. de Novion and P. Convert, *Acta Metall*. **30**: 1769 (1982).

14. P.A.P Lindberg and L.I. Johansson, *Surf. Sci.* **194**: 199 (1988).

15. G.R. Gruzalski, S.C. Lui and D.M. Zechner, *Surf. Sci*. **239**: L517 (1990).

16. M. Weiner and R.E. Watson, *Phys. Rev.* **29B**: 3001 (1984).

17. M. Aono, Y. Hou, R. Souda, C. Oshima, S. Otani and Y. Ishizawa. *Phys. Rev. Letters* **50**: 1293 (1983).

18. N. Matsuda, H. Mori, K. Hoshino and M. Watabe, *J. Phys. (Condensed Matter)* **3**: 827 (1991).

19. A. Meyer, *Z. Phys. Chem.* Bd1 **56**: 519 (1988).

20. S.P. Phillpot, D. Wolf and S. Yip, *MRS Bulletin* **15**: 38 (1990).

21. G. Bilalbegovic and E. Tosatti, *Phys. Rev.* **B48**: 11240 (1993).

22. S. Kennou, *J. Appl. Phys.* **78**: 587 (1995).

23. J. Redinger, R. Eibler, P. Herzig, A. Neckel, R. Podloncky and E. Wimmer, *J. Phys. Chem. Solids* **46**: 383 (1985).

24. M. Aono, Y. Hou, R. Souda, C. Oshima, S. Otani and Y. Ishizawa, *Phys. Rev. Letters* **50**: 1293 (1983).

25. N. Eustathopoulos, D. Chatain and L. Courdurie, *Mater. Sci. Eng.* **A135**: 83 (1991).

26. J.P. Dekker, P.J. van der Put, H.J. Veringa and J. Schoonman, *J. Electrochem. Soc.* **141**: 787 (1994).

27. H. Hochst, R.D. Bringans, P. Steiner and Th. Wolf, *Phys. Rev. Letters* **50**: 7183 (1982)

28. W. Lengauer, *J. Less-Common. Met.* **125**: 127 (1986).

29. W. Lengauer and O. Ettmayer, *J. Less-Common. Met.* **120**: 153 (1986).

30. X.B. Zhou and Th.M. De Hosson, *Acta Mater.* **44**: 421 (1996).

Table I. Contact Angles, Atomic Distances, Apparent Surface Diffusion Parameters of Liquid Cobalt and Copper, and Work Functions for Selected Carbides and Metals

Liquid Co and Cu at T_m and Carbide	θ_e, deg Refs. 10,11	L (min), nm [110] Refs. 12,13	L (max), nm [100] Refs. 12,13	D_S+D_r (min) $m^2/s \times 10^{-8}$	D_S+D_r (max) $m^2/s \times 10^{-8}$	ϕ, eV for clean surfaces Mc_x , Mn_x ($\times$ = 0.8-1.0 face (100) Refs. 14–16	ϕ, eV at an exposure of 10 L* of O_2 , Mc_x (x = 0.8-1.0) face (100) Ref. 14
Co Liquid	—	0.256	0.256	—	—	5.0	—
TiC	30	0.308	0.437	11.8	16.6	4.1	5.8
ZrC	35	0.334	0.472	12.1	17	3.5	4.7
HfC	35	0.318	0.45	11.5	16.2	4.63	NA**
VC	10	0.298	0.422	13.0	18.2	4.3	5.8
NbC	11.5	0.319	0.449	13.8	19.3	4.1	4.6
TaC	10	0.317	0.449	13.8	19.4	4.38	NA
Cu liquid	—	0.257	0.257	—	—	4.7	
$TiC_{0.98}$	110	0.308	—	—	—		
$TiC_{0.70}$	95	0.306	—	—	—		
$TiC_{0.60}$	50	0.305	0.434	6.5	9.3		
$TiC_{0.50}$	5	0.304	0.433	0.1	14.4		

* 1 L (Langmuir) = 10^{-6} Torr sec
**Not Available.

Table II. Composition, Structural Parameters of TiN_x and $Ti(N,O)_x$ Ceramics, and the Work Function ϕ

Composition	Lattice Parameter, nm cubic, B1	Sample/ϕ, eV Ref. 27	Composition	Interatomic Distances, nm rhombohedral			
$TiN_{0.96}$	0.4240 ± 0.0003	$TiN_{0.99}/\phi = 3.79$	Ti_3N_{2-x} Ref. 28	0.2401	0.2350	0.2213	0.1865
$TiN_{0.85}$	0.4225 ± 0.0002	$TiN_{0.80}/\phi = 3.66$	Ti_4N_{3-x} Ref. 29	0.2429	0.2412	0.2356	0.2188
			$TiN_{0.75}O_{0.08}$	0.2439	0.2239	0.2165	0.1750
Ti		4.3	$TiN_{0.65}O_{0.18}$	0.2379	0.2354	0.2160	0.1707

Table III. Contact Angles, Apparent Surface Diffusion Parameters of Liquid Titanium, Determined at 1973 K (determined in the present work), Work Function for Titanium Nitride and Oxynitride

Nitride	θ_e, deg	L (min), nm	D_S+D_r m^2/s, $\times 10^{-8}$
Ti Liquid	—	0.220 (Ti–Ti)	—
$TiN_{0.96}$	22	0.2998 (N–N)	19.7
$TiN_{0.85}$	15	0.2987 (N–N)	20.4
$TiN_{0.75}O_{0.08}$	35	0.2407 (N–N)*	17.0
$TiN_{0.60}O_{0.18}$	38	—	—
Al_2O_3	42**		

* Ref. 28
** Ref. 30

FIGURE CAPTIONS

Fig. 1. Schematic representation of wetting phenomena of liquid metal on substrate with indication of the quasi-solidlike skin formation at the interface.

Fig. 2. The atomic geometry of carbide (001) surface [Ref. 17].

Fig. 3. X-ray diffraction spectra from $TiN_{0.96}$ (A), $TiN_{0.75}O_{0.08}$ (B) and $TiN_{0.60}O_{0.18}$ (C).s

Figure 1

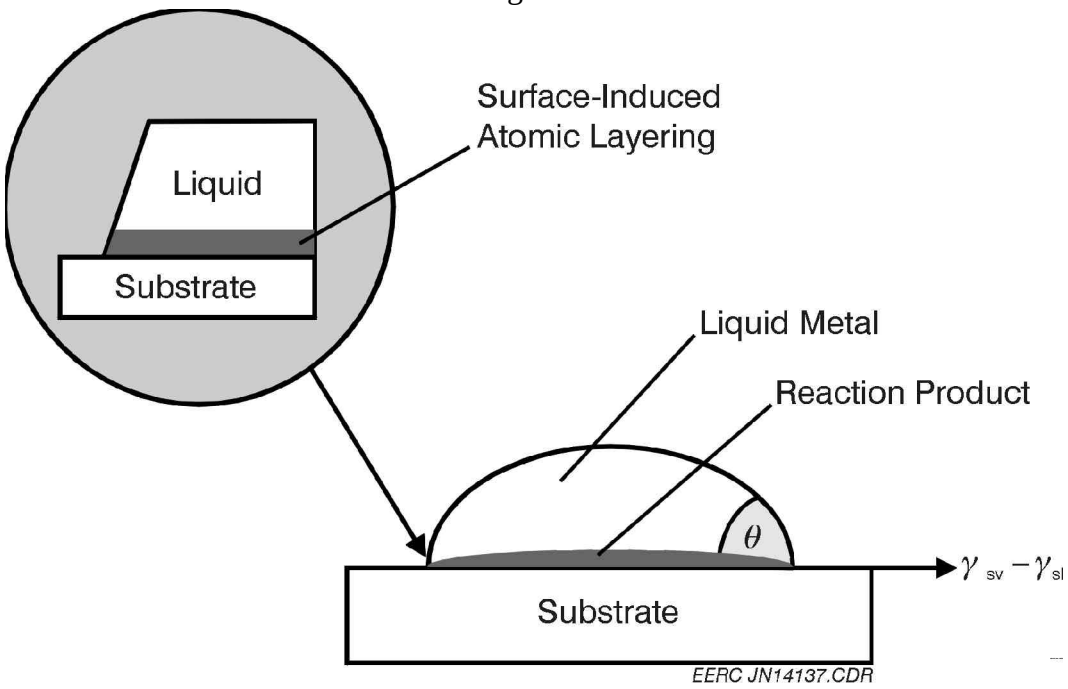

Figure 2

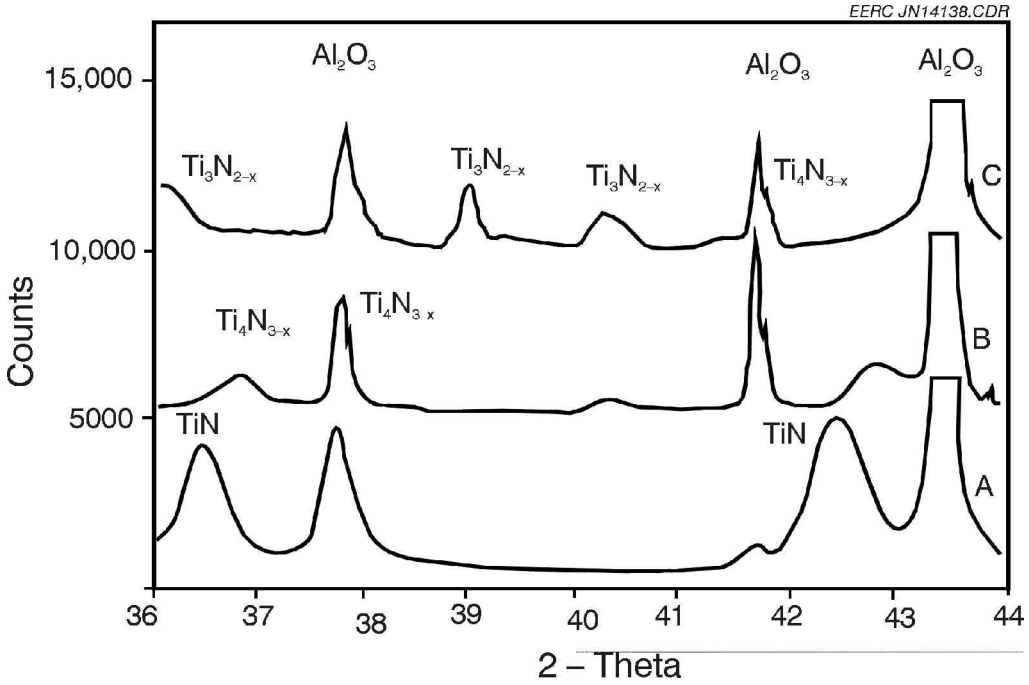

Figure 3

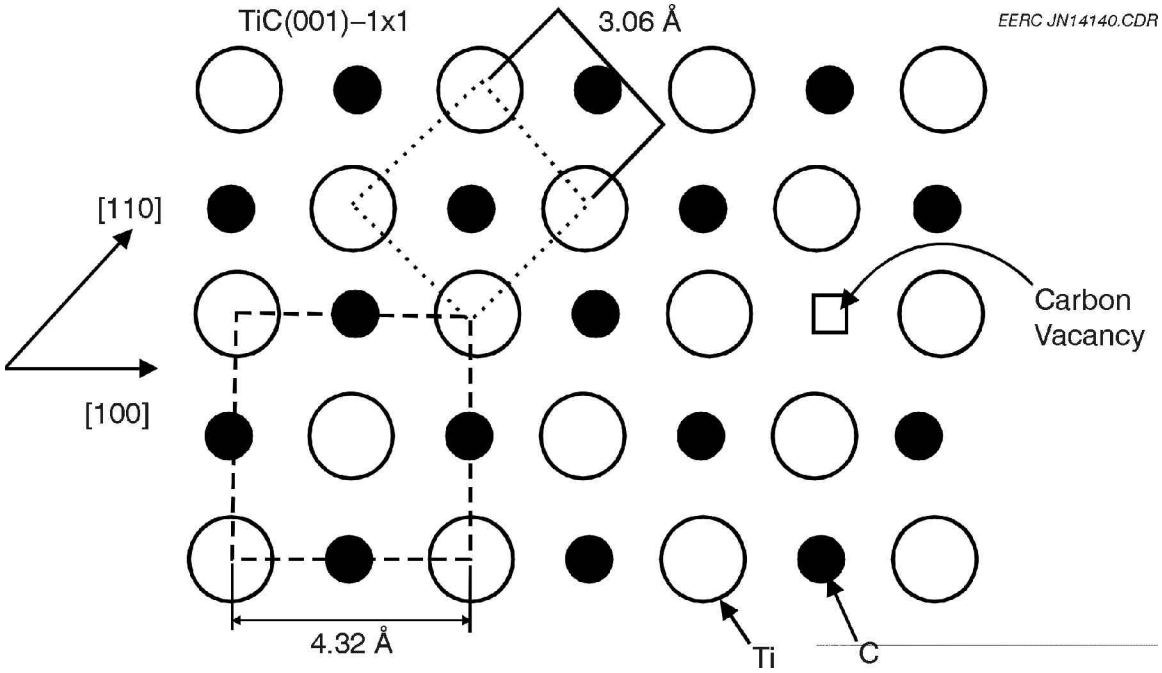
TiC(001)–1x1
3.06 Å
EERC JN14140.CDR
[110]
[100]
Carbon
Vacancy
4.32 Å
Ti
C